



# The influence of temporary hydrogenation on ECAP formability and low cycle fatigue life of CP titanium

A. Czerwinski<sup>a</sup>, R. Lapovok<sup>a,\*</sup>, D. Tomus<sup>a</sup>, Y. Estrin<sup>a,b</sup>, A. Vinogradov<sup>c</sup>

<sup>a</sup> ARC Centre of Excellence for Design in Light Metals, Department of Materials Engineering, Monash University, Clayton, Vic, Australia

<sup>b</sup> CSIRO Division of Process Science and Engineering, Clayton, Vic, Australia

<sup>c</sup> Department of Intelligent Materials Engineering, Osaka City University, Osaka, Japan

## ARTICLE INFO

### Article history:

Received 19 August 2010

Received in revised form

24 November 2010

Accepted 26 November 2010

Available online 4 December 2010

### Keywords:

CP Ti powder

ECAP

Hydrogenation

Tensile ductility

Fatigue

## ABSTRACT

It is generally believed that thermo-hydrogen processing has a beneficial effect on tensile ductility and fatigue properties of titanium. This study was concerned with investigating whether this also applies to titanium of commercial purity (CP) with an ultrafine-grained structure obtained by equal-channel angular pressing (ECAP). It was shown that despite the possibility to manipulate the microstructure of titanium the thermo-hydrogen processing offers, temporary hydrogenation was not able to improve ductility and low cycle fatigue life of CP titanium over the levels achievable by straight ECAP.

© 2010 Elsevier B.V. All rights reserved.

## 1. Introduction

Ultrafine-grained titanium obtained by severe plastic deformation (SPD) exhibits yield strength significantly improved over that of coarse grained material. An increase in the fatigue limit paired with very little deterioration of fatigue performance in the low cycle regime is also observed [1]. These results give promise that improvement of both the high cycle and the low cycle fatigue properties of titanium by SPD-induced grain refinement is possible. This is very encouraging, as a vast majority of materials manufactured by SPD [2,3] exhibit degradation of fatigue resistance in the low cycle fatigue regime. Apparently, this effect, which is believed to be associated with reduced ductility after SPD [3,4], can be avoided for ECAP-processed titanium.

Alloying with hydrogen has been shown to enhance the ductility of certain titanium alloys in a temperature range suitable for improving hot workability [5,6]. The high diffusivity of hydrogen in titanium has made it possible to exploit this fact in a technique known as thermo-hydrogen processing (THP). THP involves hydrogenation by controlled diffusion, followed by thermomechanical processing and subsequent vacuum dehydrogenation. Improvements to the microstructure and the properties of titanium alloys

(notably, in their hot workability) by THP have been widely discussed in literature [7–9].

The improvement in hot workability by THP is based on the fact that hydrogen stabilises the more ductile  $\beta$  phase and expands the range of  $\alpha + \beta$  phase stability in Ti. Critically, the  $\alpha$  to  $\beta$  transformation temperature is decreased from 882 °C in pure titanium to 300 °C at the eutectoid point; i.e. for a hydrogen concentration of ~40 at.%, Fig. 1 [10]. This is important for performing SPD without fracture at moderate temperatures as a large volume fraction of the  $\beta$  phase ensures the formability required for SPD at temperatures as low as 300 °C. Cooling of the hydrogen-containing  $\alpha$  and  $\beta$  phases below the eutectoid temperature results in the transformation of the remaining  $\beta$  phase into the  $\alpha$  phase and the  $\delta$  phase, one of several hydrides that can form. Subsequent dehydrogenation results in  $\delta$  phase decomposition and promotes the formation of microstructures with either equiaxed or acicular grains [11].

This study aims to explore whether the expected benefits of the technique with regard to room temperature ductility can be achieved with the ultrafine-grained CP titanium prepared by ECAP, with an ultimate goal of enhancing the low cycle fatigue life. The THP parameters and their effect on ECAP formability and low cycle fatigue behaviour of the ECAP-processed material will be reported.

## 2. Materials and experimental procedure

Commercial purity titanium (Grade 2–0.07%Fe, 0.15%O, 0.01%N, 0.01%C, 0.0% $\text{H}$ ) was purchased as a 10 mm diameter round bar, annealed at 704 °C for 1 h and air

\* Corresponding author.

E-mail address: [rimma.lapovok@eng.monash.edu.au](mailto:rimma.lapovok@eng.monash.edu.au) (R. Lapovok).

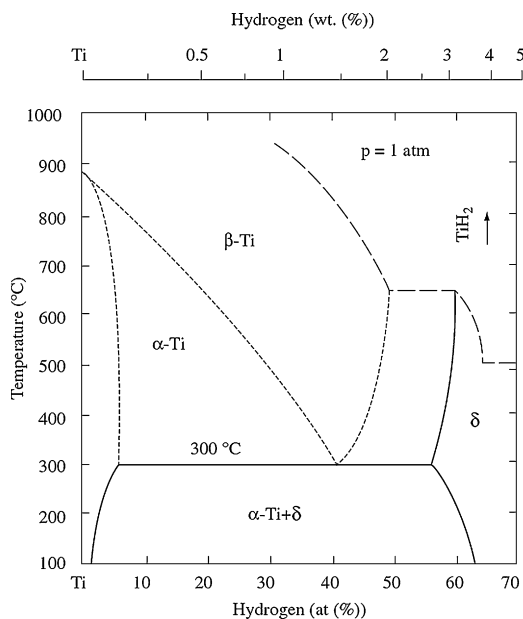


Fig. 1. Ti–H binary phase diagram (after [10]).

cooled. Before fatigue testing, samples were either ECAP processed or first hydrogenated and then ECAP processed at different temperatures. The experimental schedule used is summarised in Fig. 2.

Based on the theoretically estimated time required to achieve a sufficiently uniform hydrogen concentration across a 10 mm diameter billet, the procedure for hydrogenation and dehydrogenation was developed. Hydrogen alloying was performed at 700 °C for 15 min, 1 h and 4 h in an induction heated alumina tube furnace under a flowing supply of 20% hydrogen in argon gas [12]. Billets of 36 mm length (two at a time) were treated in an alumina combustion boat. After inserting the boat into the centre of the heating region and sealing the furnace, the atmosphere inside the furnace was purged three times. This was achieved by repeatedly filling it with hydrogen in argon gas before closing the gas source and expelling the gas using a vacuum pump. The rate of heating and cooling was limited by the capabilities of the furnace. A long heating time of approximately 2 h was used and cooling was conducted at a natural rate for the furnace. Billets were kept in the furnace during the entire heating and cooling cycle to minimise surface oxidation.

Dehydrogenation was carried out in an induction heated alumina tube furnace under a medium vacuum of  $\sim 7.5 \times 10^{-2}$  Torr with the remaining atmosphere made up by a flow of inert argon gas. Dehydrogenation of UFG samples with all ECAP histories used was performed at 500 °C for 1 h, using a heating rate of  $10^\circ\text{C min}^{-1}$  and cooling to ambient temperature at  $3^\circ\text{C min}^{-1}$ . As with hydrogenation, samples were placed in the centre of the heating zone of the furnace in an alumina combustion boat.

ECAP of titanium samples was performed at three temperatures, 300, 400 and 500 °C, using a rig designed and manufactured at Monash University. The setup features controlled forward and backward pressures and velocities of punches, as described in detail elsewhere [12,13]. Four ECAP passes were carried out using a die

with cylindrical channels intersecting at an angle of  $90^\circ$ . Pressing was performed at forward and backward pressures of 1800 MPa and 100 MPa, respectively, following route B<sub>c</sub>, which involves rotating the billet by  $90^\circ$  about the longitudinal axis between passes. The die channels and the billets were coated with an even layer of graphite lubricant releasing agent prior to each pass. Samples were water quenched from the working temperature following each pass.

X-ray diffraction (XRD) was used to obtain both qualitative and quantitative information about the phases present in titanium following each stage of processing. The experiments were performed using a Philips diffractometer equipped with a Cu-K $\alpha$  radiation source operating at 40 kV and 25 mA. Samples were mounted in a wide angle goniometer and readings were taken over a  $2\theta$  range of  $30^\circ$ – $90^\circ$  at a rate between  $1$  and  $2^\circ\text{C min}^{-1}$  using step intervals of  $0.02^\circ$ . The range was chosen to encompass the most prominent peaks produced by constructive scattering from crystallographic planes in  $\alpha$ ,  $\beta$  and  $\delta$  phases.

Vickers hardness and microhardness tests were performed using loads of 5 kg and 500 g, respectively. Measurements were performed on flat surfaces following grinding with silicon carbide paper of 800 grit or finer. All hardness values reported are based on the average of five manually measured indentations.

Reflected light optical microscopy was used to examine the microstructure of samples. Samples were prepared by a three stage, water lubricated, grinding process using progressively finer grades of silicon carbide paper (320, 800 and 1200 grit). Fine-polishing was performed using a suspension of colloidal silica (Struers OP-S) in an aqueous solution of 6 vol.% hydrogen peroxide. Microstructures were observed using both polarised light in the non-etched form and following etching with Kroll's reagent (3 vol.% hydrofluoric acid, 6 vol.% nitric acid in water).

Ductility data was based on tensile tests performed using 5 kN static load cell mounted to a screw-driven Instron 5500R machine. Sub-sized cylindrical specimens with a cross-sectional area of  $2\text{ mm}^2$  were tested in tension with a constant cross-head velocity corresponding to an initial strain rate of  $2 \times 10^{-3}\text{ s}^{-1}$ .

The fatigue tests were carried out in air at room temperature, using smooth sub-sized specimens with a  $2.4\text{ mm} \times 2.4\text{ mm} \times 5\text{ mm}$  dimensions. The samples were mechanically polished using an  $0.5\text{ }\mu\text{m}$  diamond compound. A hydraulic Shimadzu testing frame was operated at 10 Hz under sine-wave load control at stress amplitudes  $\Delta\sigma/2$  varied in the range from 350 to 600 MPa.

### 3. Results and discussion

#### 3.1. Characterisation of as-received material

XRD analysis of the as-received CP titanium confirmed that it had an  $\alpha$  phase structure. A trace amount of titanium oxide ( $\text{TiO}_2$ ) formed on the surface of the test sample was also identified, Fig. 3a. The intensity of the (002) diffraction was more than three times higher than that of the (101) diffraction, which can be attributed to a preferred crystallographic orientation imparted on the material by extrusion.

The microstructure of the as-received titanium, Fig. 3b, consisted predominantly of equiaxed grains with an average diameter of  $36 \pm 2\text{ }\mu\text{m}$  and a smaller fraction of plate-like grains. The equiaxed microstructure is typical of that expected for a cross-section of an extruded and subsequently annealed rod. The Vickers hardness of the as-received material was  $177 \pm 2$  (HV0.5) and the tensile strength and ductility (averaged over two specimens) were  $535 \pm 3\text{ MPa}$  and  $32 \pm 2\%$ , respectively.

#### 3.2. Indirect experimental measurements of hydrogen concentration profile

The characteristic time it takes for hydrogen to diffuse through a cylindrical specimen of radius  $r$  can be estimated [14] as  $t \cong r^2/4D$ , where  $D$  is the diffusivity. The hydrogen diffusivity in  $\alpha$ -titanium at temperature  $T$  is given by [15],

$$D = 1.8 \times 10^{-6} \exp\left(-\frac{12380\text{ J mol}^{-1}}{RT}\right) \text{ m}^2 \text{ s}^{-1}$$

where  $R$  is the gas constant. On this basis, an extremely short hydrogenation time of the order of 5 s would be required for a 10 mm diameter billet at the temperature of 700 °C. Experimental evidence tells us a different story, suggesting that penetration of hydrogen into a billet takes a much longer time, see below.

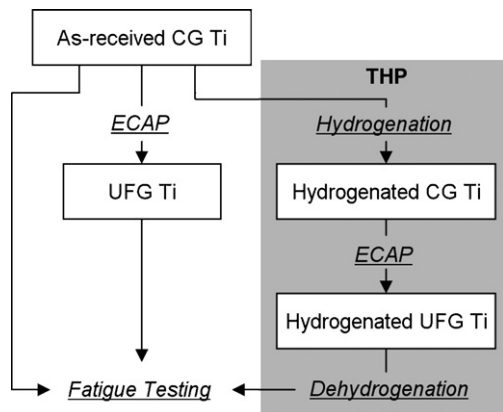
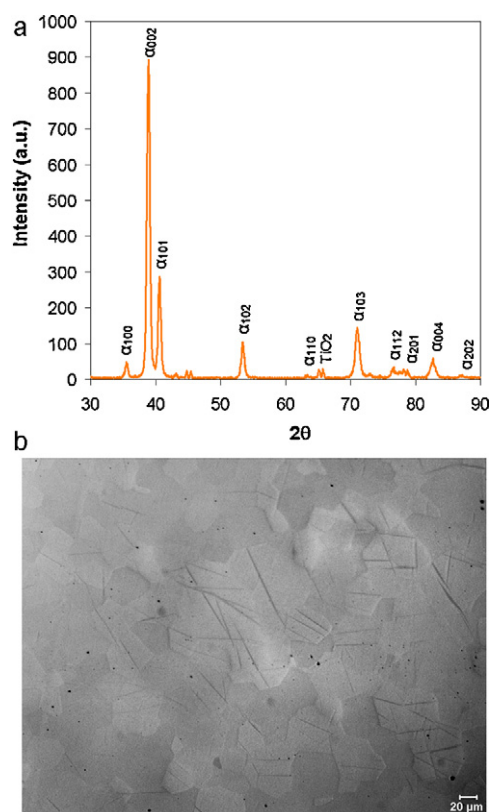


Fig. 2. Schematic of experiments. Shaded area indicates THP regime (CG = coarse grained, UFG = ultrafine grained).



**Fig. 3.** Characterisation of as-received CP Ti (a) XRD spectrum; (b) optical micrograph of polished sample.

Alloying of Ti billets with hydrogen was performed at 700 °C for three different times: 15 min, 1 h and 4 h. Hardness (assumed to be related to local hydrogen concentration) was measured along several diametric lines in cross-sections taken from the middle of the billets. The data revealed that diffusion occurred at a markedly slower rate than that predicted by the above estimate. This can be seen in a pronounced gradient of the hardness profile curve following hydrogenation at 700 °C for 15 min, Fig. 4a, supported by the XRD spectrum, Fig. 4b. The hardness in the centre of a billet cross-section approaches that of the coarse grained material, which is indicative of a low hydrogen concentration in this area. This may be seen as an indication that diffusion of hydrogen into the bulk of the specimen is hindered by an oxide layer on the surface of Ti.

Uniformity of the hardness profiles across the billets treated for both 1 h and 4 h suggest complete hydrogenation, Fig. 5a. The difference in the overall hardness levels between the billets that had experienced hydrogenation times of 1 h and 4 h may be explained by a greater stress relief in the extruded billet after 4 h at 700 °C. The reduced hardness observed following the 4 h exposure cannot be attributed to the presence of a larger fraction of residual  $\beta$  phase as this was ruled out by XRD measurements, Fig. 5. This is not unexpected given the low cooling rate employed. Similarly, micrographs do not reveal any significant difference in grain size between the two samples and thus discount any influence of grain growth, (described in Section 3.3).

### 3.3. Microstructure of hydrogenated titanium

Micrographs obtained from a region near the middle of a sample hydrogenated for the various times are shown in Fig. 6. They reveal a highly acicular, plate-like structure, particularly in the case of the two samples held for longer hydrogenation times, Fig. 6b and c. In both cases the large, light coloured plates in these images corre-

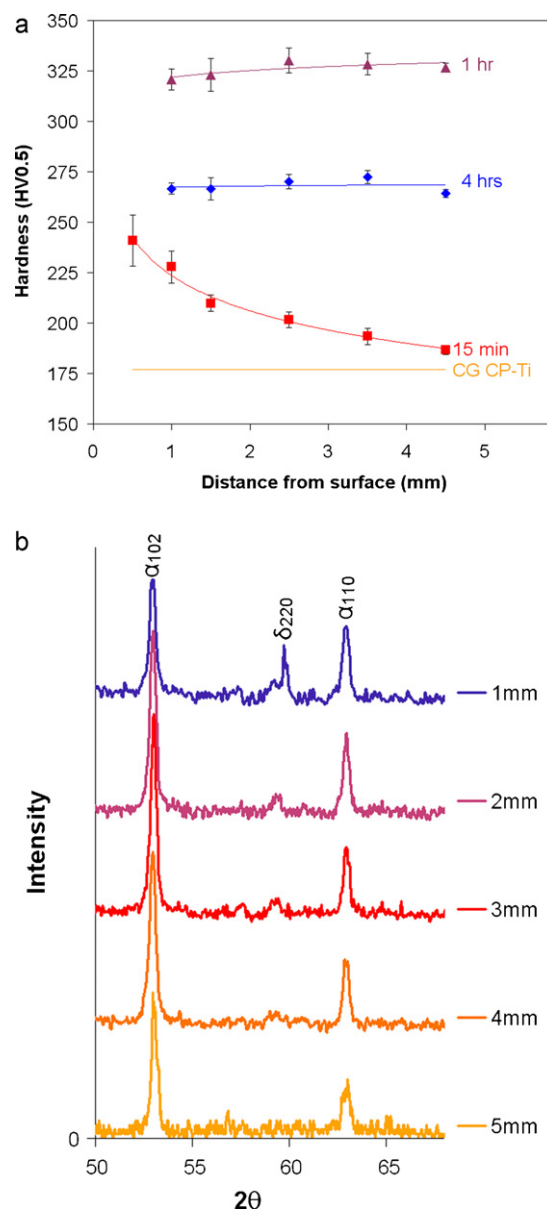


**Fig. 4.** Experimental characterisation of the hydrogenation profile. (a) Vickers hardness vs. distance from the specimen surface for different hydrogenation times; (b) XRD spectrum at five different distances from the specimen surface for sample hydrogenated for 15 min at 700 °C.

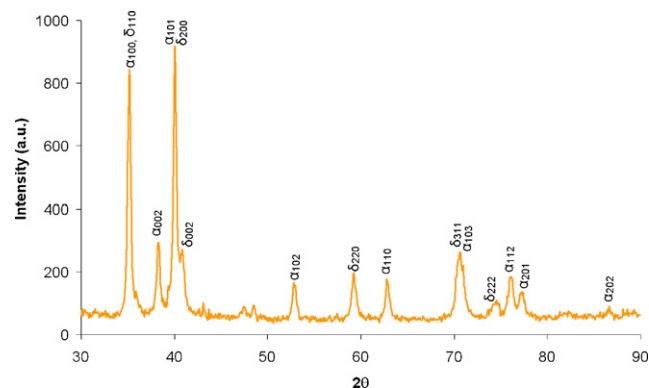


**Fig. 5.** XRD spectrum corresponding to the middle of a billet following hydrogenation for 1 h at 700 °C.



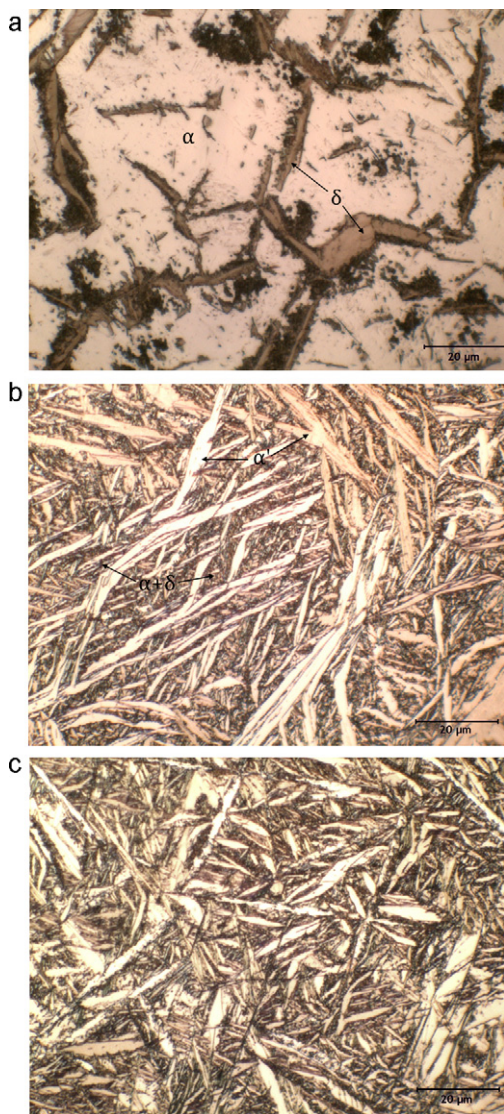


**Fig. 6.** Microstructure near the middle of billets hydrogenated for: (a) 15 min; (b) 1 h; (c) 4 h.

spond to primary  $\alpha$  phase ( $\alpha'$ ) and, interestingly, have a virtually identical average plate thickness of  $2.2 \mu\text{m}$ . These plates form preferentially along  $\beta$  phase grain boundaries while heating in, and cooling through, the  $\alpha + \beta$  region of the phase diagram [10]. The alternating light and dark regions between  $\alpha'$  plates represent a eutectic  $\alpha$ -Ti and  $\delta$  hydride structure. It is much finer than the  $\alpha'$  plates and is once again roughly the same size in both samples.

The predominantly  $\alpha$  phase structure following a treatment time of 15 min, Fig. 6a, is attributed to a lower concentration of hydrogen. The  $\alpha$  phase present in the as-received structure has remained largely untransformed; it has only become hydrogen-enriched during heating. Cooling below  $300^\circ\text{C}$  results in the formation of hydride plates mainly along grain boundaries.

The variation in the microstructure across a sample hydrogenated for 15 min can be seen in Fig. 7. It shows the transition from a microstructure resembling that of the 1 and 4 h samples at the surface to one consisting primarily of untransformed  $\alpha$  phase in the middle of the billet.

Based on these experimental results, a hydrogenation time of 1 h was selected as most appropriate for achieving an effectively uniform hydrogen concentration throughout a billet at the hydrogenation temperature of  $700^\circ\text{C}$ .

**Table 1**

Summary of hardness and XRD results for ECAP-processed titanium.

$T_{\text{ECAP}} (^{\circ}\text{C})$	Hardness (HV5)	Relative wt. fraction of $\delta$
Before ECAP	$320 \pm 4$	1
300	$262 \pm 1$	0.59
400	$250 \pm 2$	0.59
500	$244 \pm 1$	0.60

#### 3.4. ECAP of hydrogenated titanium

ECAP of hydrogenated Ti billets was performed at a number of different temperatures in order to screen the various processing conditions and check whether hydrogenation is beneficial for SPD processing. Furthermore, the potential for achieving *in situ* dehydrogenation by altering the temperature was explored.

The microstructures of billets after ECAP processing are shown in Fig. 8. Optical micrographs clearly show that the large shear strains imposed on the material have imparted a degree of orientation to the plate-like  $\alpha'$  phase and have given rise to an almost lamellar morphology. The microstructure resulting from ECAP at  $300^\circ\text{C}$  is very similar to that resulting from ECAP at  $400^\circ\text{C}$ , Fig. 8a. The thickness of  $\alpha'$  plates has actually increased slightly during ECAP processing, with values of  $3.4 \pm 0.3 \mu\text{m}$  and  $3.9 \pm 0.2 \mu\text{m}$  for the  $300^\circ\text{C}$  and  $400^\circ\text{C}$  processing, respectively. The  $\alpha'$  phase size after ECAP at  $500^\circ\text{C}$  is fine by comparison, Fig. 8b, with an average thickness of  $1.2 \pm 0.1 \mu\text{m}$ . The trend observed in the darker regions of  $\alpha$  titanium and  $\delta$  hydride surrounding  $\alpha'$  plates is quite different. Equiaxed grains of  $860 \pm 35 \text{ nm}$  average size, with an appreciable fraction of noticeably smaller grains at their boundaries, are visible following ECAP at  $500^\circ\text{C}$ . The microstructure in these regions cannot be resolved by optical microscopy in the billets processed at the lower ECAP temperatures.

The different microstructures observed following ECAP at the highest temperature can be attributed to a number of factors. Firstly, the finer nature of the  $\alpha'$  plates is explained by their increased decomposition into  $\alpha + \beta$  at  $500^\circ\text{C}$ . The expected reduction of flow stress due to the thermally activated nature of plastic flow is compounded in hydrogenated CP titanium by the fact that the ratio of soft  $\beta$  to hard  $\alpha$  phase increases with temperature. Indeed, Salishchev et al. have reported that in hydrogenated CP titanium grain refinement becomes more effective for lower ECAP temperature [16]. The finer microstructure was observed down to  $400^\circ\text{C}$ , the lower limit of their tested range, and it was attributed to dynamic recrystallisation. The fact that recrystallisation is driven by grain boundary diffusion means it requires a higher critical strain to set in at lower temperature. It is nevertheless observed due to the large fraction of relatively mobile grain boundaries with large misorientations formed by ECAP. However, given that recrystallisation is more prevalent at higher temperature it is also possible that accelerated coarsening of recrystallised grains at  $500^\circ\text{C}$  may contribute to the coarser microstructure.

XRD was used to observe changes in hydride content resulting from ECAP at different temperatures, Fig. 9. It indicates that the intensity of the  $\delta$ -(2 2 0) diffraction peak remains fairly consistent with respect to the average intensity of the (1 0 2) and (1 1 0) peaks for  $\alpha$ -Ti. This information, based on the integrated intensities, is summarised in Table 1. Comparison with material that has not been refined by SPD suggests that although appreciable dehydrogenation takes place, the processing temperature does not have a significant effect on the final hydride concentration. Although holding samples at elevated temperature for longer periods may lead to more hydrogen removal, this would also be accompanied by some grain growth. The possibility of achieving *in situ* dehydrogenation was discounted given the well documented ability to



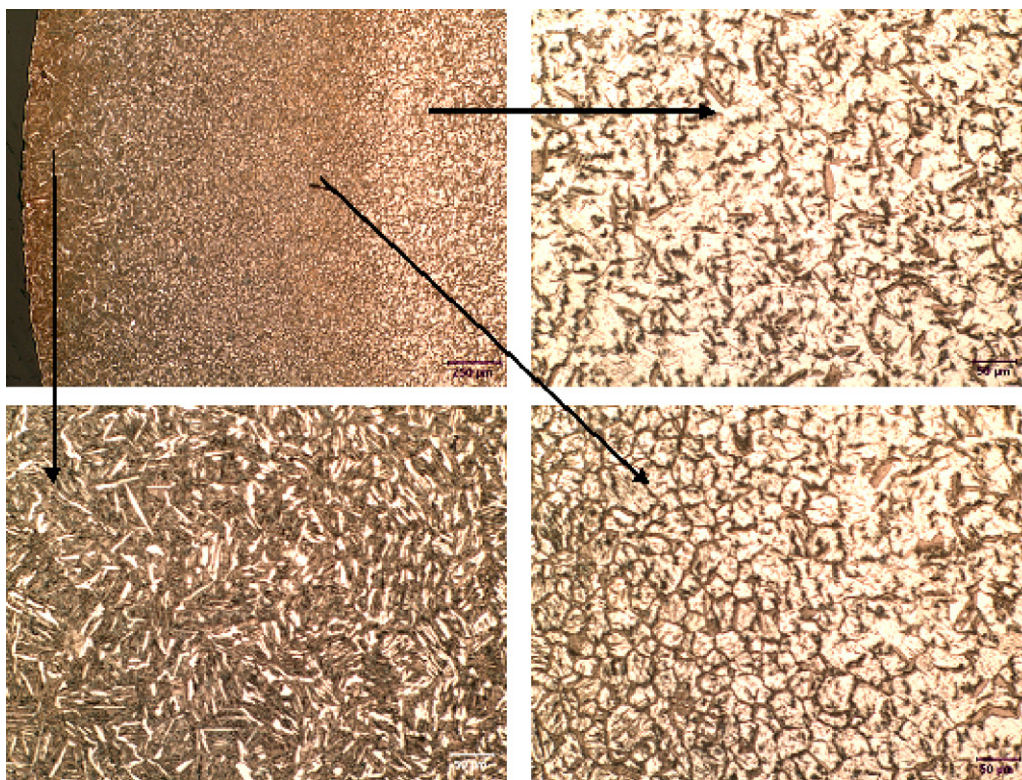


Fig. 7. Variation in microstructure across a Ti billet hydrogenated for 15 min shown in optical micrographs taken at (a) low and (b)–(d) high magnification.

accelerate removal in a vacuum environment. It should be noted that the absence of  $\beta$  phase peaks in the XRD spectra indicates that the quenching rate used was too slow for the high temperature phases to be retained.

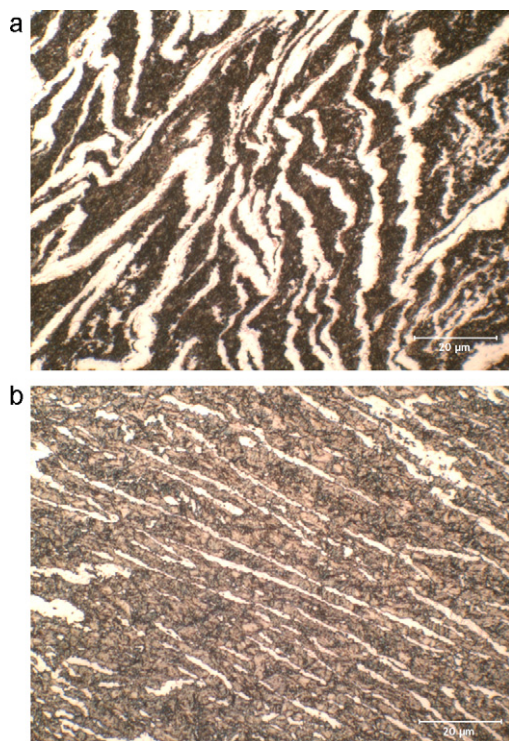


Fig. 8. Microstructure of Ti hydrogenated for 1 h at 700 °C and processed by ECAP at (a) 400 °C; (b) 500 °C.

The results in Table 1 also reveal that irrespective of the magnitude of the uniform hydride fraction, the hardness of samples decreases with increased deformation temperature. This is consistent with expectations of grain coarsening at higher temperature and increased microstructure refinement at lower temperature mentioned previously. Surprisingly, hardness has been significantly reduced by ECAP processing relative to the starting hydrogenated material. This contradicts typical observations for SPD processed materials but is consistent with the diminished relative fraction of  $\delta$  phase. Despite the reduced hardness, tensile tests revealed a brittle failure mode for all samples that have undergone ECAP. This highlights the need to perform vacuum dehydrogenation.

### 3.5. Mechanical properties after dehydrogenation

To avoid grain coarsening, a low dehydrogenation temperature of 500 °C was used. It is based on results reported in [16] where a minimum dehydrogenation temperature of 500 °C was suggested

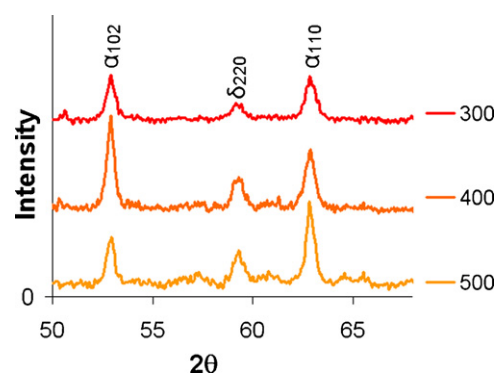
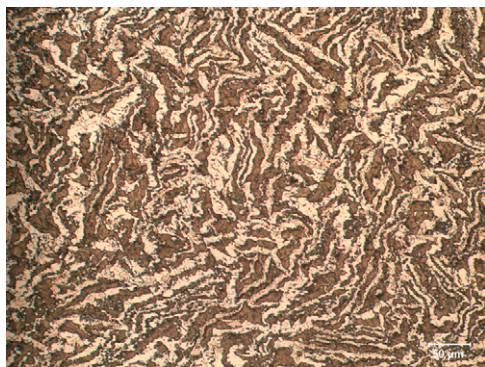


Fig. 9. XRD spectrum of titanium processed by ECAP at different temperatures.





**Fig. 10.** Microstructure after ECAP at 500 °C after vacuum dehydrogenation for 1 h at 500 °C.

based on differential thermal analysis of titanium hydride powder. Samples were heated to 500 °C and held at that temperature for 1 h on the basis that complete dehydrogenation of  $TiH_2$  powder was reported to occur within 50 min at this temperature [17].

The microstructure of samples processed by four passes of ECAP at 500 °C followed by dehydrogenation is shown in Fig. 10. It is very similar to the bimodal microstructure observed just after ECAP, Fig. 8b, and consists of slightly coarsened elongated  $\alpha$  phase of several microns thickness surrounded by an equiaxed ultrafine grained matrix.

The hardness of  $218 \pm 2$  HV5 recorded for the material is consistent with the slight coarsening observed as it falls between that of the ultrafine grained sample prior to dehydrogenation ( $244 \pm 1$  HV5) and that of the coarse grained CP-titanium ( $169 \pm 3$  HV5). Tensile curves for coarse grained, ultrafine grained (four ECAP passes at 300 °C) and THP (hydrogenation, four passes of ECAP at 500 °C or four passes of ECAP at 300 °C, dehydrogenation) samples are shown in Fig. 11. It can be seen that despite the lower ductility of the THP sample compared to coarse grained titanium, the character of the tensile curve is similar in that there is still appreciable ductility after reaching the ultimate tensile stress, geometrical softening being not abrupt but rather producing a curve with the same prolonged shape. As expected, the strength of the material is reduced on account of exposure to high temperature during dehydrogenation and slight coarsening of the structure. The THP material nevertheless retains an ultrafine grained structure and its strength is higher compared to coarse grained titanium. ECAP temperature only slightly affects the strength and ductility of THP samples, though samples processed by ECAP at 500 °C have fractionally lower strength and higher ductility. This is in agreement with the hardness data in Table 1.

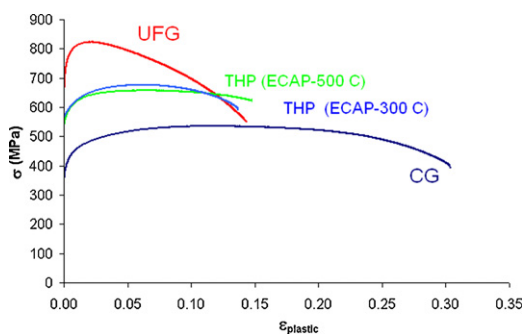


**Fig. 11.** Tensile test data for Ti treated by THP for ECAP temperatures of 300 °C and 500 °C. Tensile curves for coarse grained (CG) and ultrafine grained (UFG) titanium (after ECAP at 300 °C) are also shown for comparison.

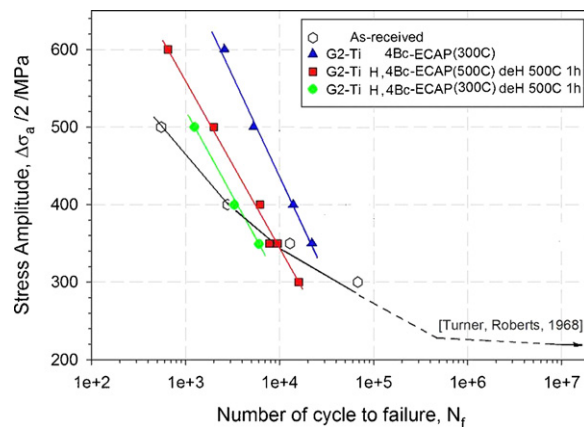


**Fig. 12.** LCF life of coarse grained Ti (rombs), ultrafine grained Ti after ECAP at 300 °C (triangles), and for Ti treated by THP with ECAP temperatures 300 °C (circles) and 500 °C (squares).

### 3.6. Low cyclic fatigue life

A property of particular interest for applications of titanium is fatigue resistance. This has been characterised using the S–N plot shown in Fig. 12 for material in the as-received condition, following ECAP and for titanium subjected to THP. At all stress amplitudes the fatigue life of THP samples appeared to be shorter than that of its ultrafine grained counterpart produced by ECAP alone. The result is not surprising as empirical proportionality between the fatigue strength and the ultimate tensile strength for monotonic loading holds for ultrafine grained metals [3]. Hence the lower tensile strength measured for material following THP also results in a lower fatigue strength, which translates to a shorter fatigue life.

It is interesting to note that ECAP at 500 °C produced samples with a longer low cycle fatigue (LCF) life than those processed by ECAP at 300 °C. This may be rationalised in terms of additional *in situ* dehydrogenation of samples during ECAP. However, the reduced fatigue life of THP samples compared to ultrafine grained samples indicates the possibility of the occurrence of residual  $\delta$  phase, which is detrimental to ductility and thus to LCF life. The tendency for improved fatigue life with increasing ECAP temperature confirms this. Therefore, despite the fact that THP treatment can significantly improve the ultrafine grained structure, no positive effect of THP on ductility and LCF life of CP titanium was found. An increase in dehydrogenation temperature above 500 °C was not possible as it resulted in restoration of a coarse grained microstructure and in stress-strain curves similar to that shown for as-received titanium in Fig. 11.

## 4. Conclusions

The hydrogenation conditions for achieving complete and uniform hydrogen alloying of CP-titanium have been determined. The hydrogenation for 1 h at 700 °C resulted in a uniform highly plate-like structure with an average plate thickness of 2.2  $\mu$ m. It formed preferentially along grain boundaries in the  $\beta$  phase during heating and cooling through the  $\alpha + \beta$  region of the phase diagram. A 15 min hydrogenation duration at 700 °C was not sufficient for uniform through-thickness alloying with hydrogen, as a gradient of microstructure from a coarse grained core to a plate-like one at the periphery of the billet was found. However, such a microstructural profile and the attendant non-uniform hardness distribution may be useful for achieving a gradient in mechanical properties akin to case hardening of steels. A longer hydrogenation time of 1 h was sufficient for producing a homogeneous microstructure and nearly uniform hardness throughout a cross-section of a billet.

Mechanical testing of THP samples has shown that temporary alloying with hydrogen helps modify the microstructure of CP titanium, resulting in a good compromise between tensile strength and ductility; it possesses ductility similar to that of coarse-grained material without sacrificing the strength obtained by grain refinement. However, the LCF life of THP samples, while being better than that for coarse-grained samples, was inferior to that of ultrafine grained material processed by straight ECAP without temporary hydrogen alloying. This is a somewhat discouraging result. It was felt, however, that despite this negative finding/connotation its publication will be useful. It is hoped that it will spare our fellow researchers working in the field future unsuccessful efforts to apply THP in a hope to improve the LCF life of ultrafine grained CP titanium.

## References

- [1] A. Vinogradov, V.V. Stolyarov, S. Hashimoto, R.Z. Valiev, *Mater. Sci. Eng. A* 318 (1–2) (2001) 163–173.
- [2] W.-J. Kim, C.-Y. Hyun, H.-K. Kim, *Scripta Mater.* 54 (10) (2006) 1745–1750.
- [3] Y. Estrin, A. Vinogradov, *Int. J. Fatigue* 32 (6) (2010) 898–907.
- [4] H.W. Höppel, M. Kautz, C. Xu, M. Murashkin, T.G. Langdon, R.Z. Valiev, H. Mughrabi, *Int. J. Fatigue* 28 (9) (2006) 1001–1010.
- [5] B.A. Kolatchev, et al., *Titanium'92 Science and Technology*, vol. 1, TMS, Warrendale, 1993, p. 861.
- [6] R.J. Lederich, et al., *Advanced Processing Methods for Titanium*, TMS-AIME, Warrendale, 1982, p. 115.
- [7] D. Eliezer, N. Eliaz, O.N. Senkov, F.H. Froes, *Mater. Sci. Eng. A* 280 (2000) 220–224.
- [8] O.N. Senkov, F.H. Froes, *Int. J. Hydrogen Energy* 24 (1999) 565–576.
- [9] F.H. Froes, O.N. Senkov, J.I. Qazi, *Int. Mater. Rev.* 49 (3–4) (2004) 227–245.
- [10] H.R.Z. Sandim, B.V. Morante, P.A. Suzuki, *Mater. Res.* 8 (2005) 293–297.
- [11] R. Lapovok, D. Tomus, V.M. Skripnyuk, M.R. Barnett, M.A. Gibson, *Mater. Sci. Eng. A* 513–514 (2009) 97–108.
- [12] R. Lapovok, D. Tomus, M.R. Barnett, M.A. Gibson, *Int. J. Mater. Res.* 12 (2009) 1727–1738.
- [13] R. Lapovok, D. Tomus, B.C. Muddle, *Mater. Sci. Eng. A* 490 (1–2) (2008) 171.
- [14] P. Shewmon, *Diffusion in Solids*, TMS, 1989.
- [15] I. Lewkowicz, *Solid State Phenom.* 49–50 (1996) 239–274.
- [16] G.A. Salishchev, M.A. Murzinova, S.V. Zharebtsov, D.D. Afonchev, S.P. Malyshcheva, *Mater. Sci. Forum* 357–359 (2001) 1223–1228.
- [17] V. Bhosle, E.G. Baburaj, M. Miranova, K. Salama, *Mater. Eng.* A356 (2003) 190–199.